Iranian Journal of Materials Forming 14 (1) (2027) 96-111

Online ISSN: 2383-0042

IJMF

Iranian Journal of Materials Forming

Journal Homepage: http://ijmf.shirazu.ac.ir



Research Article

Finite Element Evaluation of Silicone Rubber Composites for Metacarpophalangeal Joint Implants

Sahar Ziraki*, Amir Ali Ashraf, Seyed Mojtaba Zebarjad and Mohammad Jafar Hadianfard

Department of Materials Science and Engineering, School of Engineering, Shiraz University, Shiraz, Iran

ARTICLE INFO

Article history:

Received: 21 August 2026
Reviewed: 12 September 2026
Revised: 25 September 2026
Accepted: 3 October 2026

Keywords:

Metacarpophalangeal joint implant
Silicone rubber composite
Finite element analysis (FEA)
Abaqus

Please cite this article as:

Ziraki, S., Ashraf, A. A., Zebarjad, S. M., & Hadianfard, M. J. (2027). Finite element evaluation of silicone rubber composites for metacarpophalangeal joint implants. *Iranian Journal of Materials Forming*, *14*(1), 96-111. https://doi.org/10.22099/IJMF.2026.56939.1390

ABSTRACT

The metacarpophalangeal joint is one of the most important and highly mobile joints in the hand, and if it is affected by disease, it may need to be replaced with a prosthesis. However, implant fracture and mechanical degradation are important concerns. Therefore, it is important to investigate the implant's behavior. Finite element analysis (FEA) has been widely used to study the biomechanics of joints and is an effective method to predict joint motion and failure. In this study, metacarpophalangeal joint implants made from different types of silicone rubber composites, including silica nanoparticles/silicone rubber composites, polypropylene fibers/silicone rubber composites, and a hybrid composite of silica/polypropylene fibers /silicone rubber, were simulated using Abaqus to investigate stress distribution and the range of motion of the implants under specific flexion and loading conditions. The implant was subjected to flexion up to 70° and to a 0.5 N external load. The finite element analysis showed that stress in the central regions was higher than in other regions, and stress increased with increasing flexion and extension angles. Under a constant external load of 0.5 N, the P2 composite exhibited the lowest displacement, strain, and stress, with values of 3.31, 0.11, and 0.33 MPa, respectively, compared with 12.92, 0.41, and 0.55 MPa for pure silicone. The results indicate that reinforcement of silicone rubber can substantially reduce implant deformation under load, which may contribute to a longer implant lifespan.

© Shiraz University, Shiraz, Iran, 2027

1. Introduction

The joints in the human body enable movement and the performance of various physical activities on daily life. Disease or degenerative changes in the bones and cartilage, especially in middle age, along with a reduction in the natural secretion of viscoelastic fluid into the joints, have made it joint replacement increasingly necessary [1, 2]. The metacarpophalangeal (MCP) joint, which is the joint between the metacarpus and the proximal phalanx, may be damaged because of aging or arthritis, and when drugs, physiotherapy, or other nonsurgical treatments fail, arthroplasty can be considered as a last resort. In this method, the finger joint is replaced with an implant to relieve pain, restore range

* Corresponding author
E-mail address: s.ziraki@shirazu.ac.ir (S. Ziraki)
https://doi.org/10.22099/IJMF.2026.56939.1390

Published by Shiraz University. This is an open access article under the CC BY-NC-ND license (http://creativecommons.org/licenses/by-nc-nd/4.0/).

of motion, and preserve the joint's appearance [3–5]. Various types of MCP joint implants with different designs and materials have been used for many years. Among them, the Swanson implant, which is made of silicone, is one of the most widely used and accepted implants [6, 7]. In spite of overall patient satisfaction, this implant may fail over time [8]. Therefore, predicting the behavior of implants with different materials and designs can help reduce the risks associated with joint replacement. In this regard, finite element analysis (FEA) can be used to predict implant failure and evaluate range of motion [9]. In this method, the mechanical properties and behavior of the material model are converted into mathematical formulations, providing reliable approximations of real-world conditions. This approach helps identify materials and design imperfections and evaluate implant behavior [10]. In order to prevent failure, biomechanical information is essential, and FEA is widely used to study body joints. However, fewer studies have been conducted on smaller joints (i.e., metacarpophalangeal joints) compared with knee and hip replacements, which are more commonly studied and have higher success rates. Therefore, gaining a deeper insight into finger joint biomechanics, materials selection, and surgical techniques is crucial for successful joint replacement [6, 7]. For example, Kadir et al. [11] modeled an implant inserted into bone and applied a load of 1 N to the proximal interphalangeal joint to simulate flexion in Swanson and Neuflex implants. Their results showed that the Neuflex implant exhibited a greater range of motion, while the Swanson implant showed greater displacements. Similarly, Biddiss et al. [3] used geometrical models of Swanson and Neuflex implants in Ansys, and their simulation under flexion showed that the maximum stress generated in the Swanson implant was higher than that in the Neuflex implant. Soman et al. [12] imported data from a fractured finger into Mimics and designed a Swanson implant for it using Autodesk Inventor. They applied different loads and compared the stress in the implanted and intact fingers. They observed that the finger with the implant was still able to perform its function. Completo et al. [13] investigated the effect of joint flexion amplitude on bone strain, implant stress, and the risk of complications in silicone metacarpophalangeal joint arthroplasty and suggested that limiting flexion could enhance implant longevity. Kim et al. [14] investigated the biomechanical characteristics of a novel proximal interphalangeal joint (PIPJ) implant using finite element analysis and showed that the new design exhibited lower stress, strain, and moment reaction values during joint motion, indicating better biomechanical performance. Pankaj [15] focused on bone modeling and the simulation of interactions between bones and implants. Advances in imaging technology now allow the creation of customized geometries and models tailored to individual patients.

FEA has been widely used as a useful method to investigate stress distribution in implants and predict the range of motion and the risk of failure. While most existing research has focused on comparing different implant designs, which is a crucial factor in implant success, FEA can also be employed to evaluate the performance of various biomaterials used in implant fabrication. Therefore, in this study, FEA was used to simulate the metacarpophalangeal joint, and the aim was to investigate three different silicone rubber composites under conditions of flexion and applied load to study stress distribution and implant performance. Silicone rubber composites are promising candidates for finger joint implants because of their biocompatibility, mechanical properties, and reported clinical success [16]. The addition of reinforcement materials to silicone can further enhance its mechanical behavior. The results of FEA can be used to select an appropriate material and design to reduce the risks of joint replacement failure.

2. Experimental Procedure

In this study, various materials used in metacarpophalangeal implants were evaluated and compared under two conditions:

1. Flexion of implants to 70° to examine stress distribution (the functional range of motion for finger joint flexion is approximately 33-70°).
2. Applying a load of 0.5 N to investigate the range of motion.

The input data were obtained from the materials used in the author's previous studies [17]. The composite implants included polypropylene (PP) fibers (1 and 2 wt.%) and silica nanoparticles (1 and 2 wt.%) in a silicone rubber matrix. They were designated as P1, P2, S1, and S2, respectively. Moreover, a hybrid composite containing both reinforcements (referred to as SP), as well as pure silicone rubber, was used. The designation of these samples is listed in Table 1. Finite element analysis was performed using Abaqus 6.11 software.

2.1. Implant design

Implant design is a critical parameter in implant success. Pylios [18] conducted extensive research on implant designs and identified parameters that affected the implant's performance suggesting an optimal design , which is shown in Fig. 1. This design was used for the present simulation study. An angle of 30° between the metacarpal and proximal phalanx, which is the neutral position of a natural joint, was considered to reduce the induced stress.

This design has six parts, each made of materials such as polyethylene, titanium, or cobalt-chromium alloy, and polyurethane. The metacarpal and proximal stems were fitted into the medullary canal of the bone, as shown in Fig. 1. The function of the middle piece, which is made of silicone rubber, is similar to that of a one-piece implant. This part is the most prone to failure; therefore, only this component, shown in Fig. 2, was included in the simulation to evaluate stress distribution. Because the objective of this study was to investigate the mechanical response of the flexible silicone elastomeric component, the complete bone–implant assembly was simplified and only the central silicone portion of the implant was modeled. In the original implant design, the metacarpal and proximal stems are positioned within the corresponding bone structures, whereas the central silicone component acts as the flexible hinge. Therefore, the metacarpal-side end of the modeled silicone component was fixed to represent the constraint imposed by the metacarpal-side assembly, while the proximal-phalanx-side end was allowed to move to reproduce joint flexion.

2.2. Assumptions

Silicone rubber is an elastomer, and elastomers are generally considered incompressible, homogeneous, isotropic, and hyperelastic materials. The strain energy potential function is one of the commonly used mathematical models for hyperelastic materials, which have various formulations, including the Mooney-Rivlin, Ogden, Arruda-Boyce, and Neo-Hookean models, among which the Mooney-Rivlin model is most

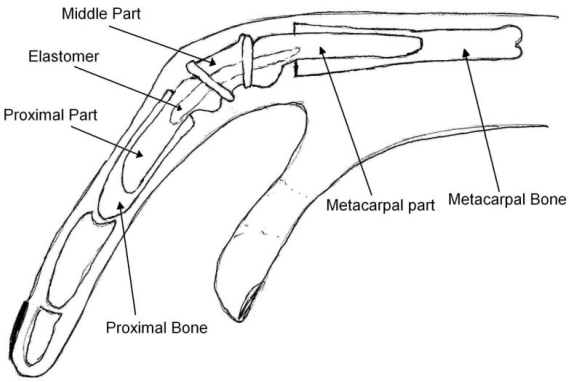


Fig. 1. Pylios design of metacarpophalangeal joint implant [18].

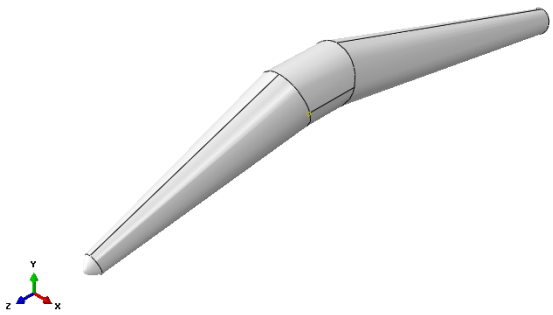


Fig. 2. Silicone elastomer part.

Table 1. Samples composition (wt.%)

Samples	Pure	S1	S2	P1	P2	SP
Silicone rubber	100	99	98	99	98	98
SiO_2	0	1	2	0	0	1
Polypropylene	0	0	0	1	2	1

commonly used [18]. Silicone rubber was modeled as a hyperelastic material using the two-parameter Mooney–Rivlin constitutive model. The strain-energy density function was defined as:

$$W = C10(I1 - 3) + C01(I2 - 3) \quad (1)$$

where W is the strain-energy density, C10 and C01 are the Mooney–Rivlin material constants, and I1 and I2 are the first and second deviatoric strain invariants, respectively. The values of C10 and C01 used in the Abaqus simulations were obtained by fitting the experimentally characterized mechanical response of the corresponding materials. The resulting parameters for each investigated formulation are reported in Table 2. The C10 and C01 parameters were determined by minimizing the sum of squared errors between the experimental engineering stress and the stress predicted by the Mooney–Rivlin constitutive equation The experimentally obtained stress–strain data were fitted using the two-parameter Mooney–Rivlin model, and the resulting model predictions were compared with the experimental data as can be seen for pure silicone rubber in Fig. 3. Good agreement was observed between the experimental stress–strain curve and the Mooney–Rivlin prediction, particularly within the strain range relevant to the finite element analysis (up to 40% strain as discussed in the Results and Discussion section).

The simulation was conducted based on the following assumptions: The metacarpal was fixed in all directions (zero degree of freedom)

- The proximal phalanx was allowed to move.
- Flexion occurred through movement of the proximal phalanx.

Based on these assumptions, the implant model was simplified as shown in Fig. 4(a). The proximal head depicted in Fig. 1 was considered in this simplified design to simulate flexion.

This simplification was adopted to isolate the mechanical response of the silicone component and to compare the effects of the different composite formulations under identical boundary conditions.

2.3. Mesh density

Four-node solid tetrahedral elements were used for meshing. Hybrid elements were employed for the incompressible material. To enhance accuracy, fine mesh refinement was used in regions of high stress concentration, particularly in the hinge part of the implant as depicted in Fig. 4(b) [11]. The mesh density in the hinge region consisted of 4589 elements. A mesh-convergence analysis was performed prior to the finite element simulations. The mesh density was progressively increased until the variation in the maximum von Mises stress between successive mesh refinements was less than 1%. The mesh satisfying this criterion was considered sufficiently refined and was subsequently used for the simulations. The direction of the applied load is shown in Fig. 4(c).

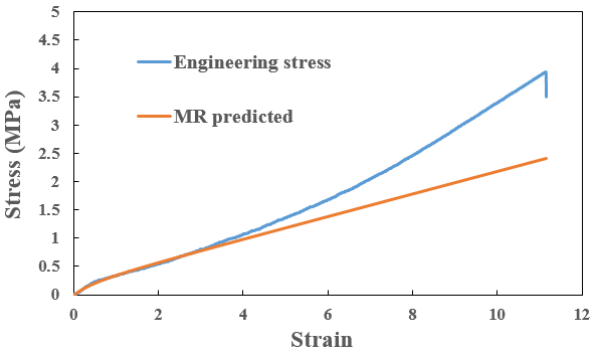


Fig. 3. Comparison between the Mooney–Rivlin (MR) prediction and the experimental stress–strain curves.

Table 2. Mooney-Rivlin constants

	Pure	S1	S2	P1	P2	SP
C10	0.099	0.134	0.225	0.213	0.304	0.259
C01	0	0	0	0	0	0

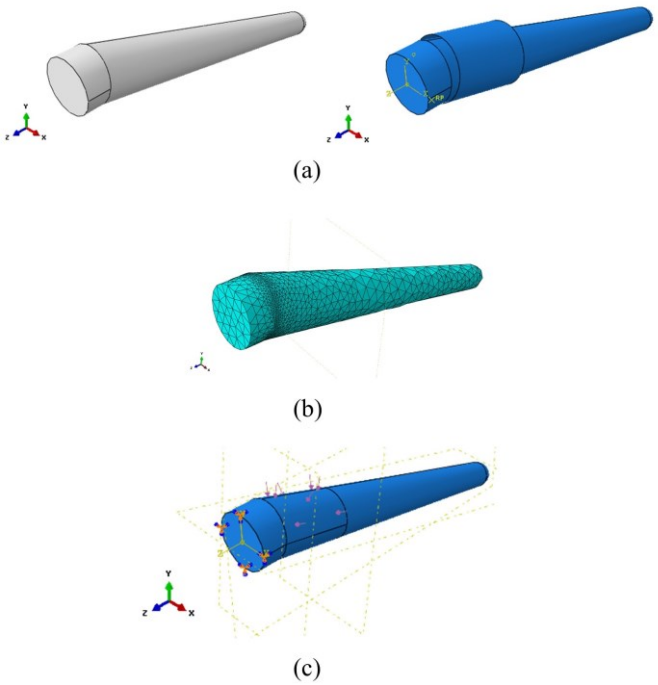


Fig. 4. Schematic representation of the (a) simplified implant model, (b) FE mesh, and (c) loading and boundary conditions applied in the FE model.

3. Results and Discussion

3.1. Stress distribution during flexion

Figs. 5 to 7 show the von Mises stress distribution in all implant samples at 70° of flexion and various joint angles relative to the 30° initial configuration. The joint angle was defined as the angle between the longitudinal axes of the metacarpal and proximal phalanx. The initial configuration of the model was set to 30° and was considered the reference position. Changes in the joint angle were measured relative to this initial configuration. An increase in the angle above 30° represents flexion, whereas a decrease below 30° represents extension relative to the initial configuration. The flexion angle is defined as the angle between the metacarpal and proximal phalanx. During flexion, the upper surface of the joint undergoes extension, while the lower surface experiences flexion. Maximum stress occurred at the highest angle of flexion, and this region is marked by arrows in Fig. 5. On the other hand, minimum stress was observed at 30° in all samples because of the initial angle between the metacarpal and proximal phalanx stems.

The increase in stress with increasing flexion is important because the hinge is also the region where clinically relevant implant damage has been reported. Recent clinical and computational studies have identified the stem–hinge region as a critical location for silicone MCP implant fracture and stress concentration [9, 13]. Thus, the present FEA result provides a material-level explanation for why reinforcement and local geometry should be considered together: increasing material strength can improve resistance to deformation, but it does not necessarily eliminate the local concentration generated by the implant geometry.

Under the same flexion or strain conditions, higher stress levels were observed in samples with stronger implant materials. As reported in previous studies, the tensile strength of S2 is higher than that of the other samples shown in Fig. 5. This is attributed to the interaction between silica nanoparticles and the polymer chains of silicone rubber, which increases the stress required to align the chains. As a consequence, S2 showed a higher stress level than the other materials. Similar results were obtained for the P2 composite, as shown in Fig. 6, which also showed a high stress level. The strength of these composites is due to efficient load transfer from the matrix to the PP fibers. Increasing the reinforcement content increases their reinforcing effect. Fig. 7 compares the stress distributions of the two composites.

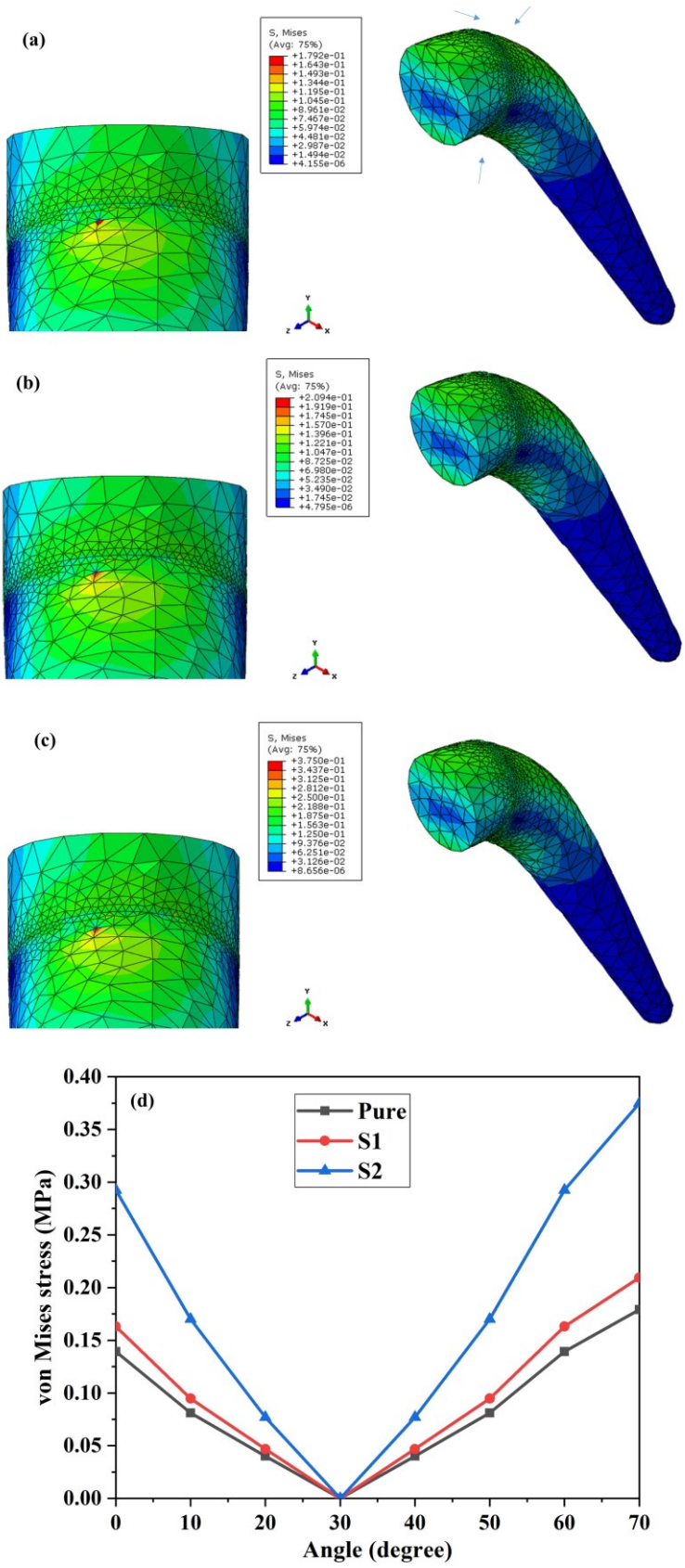


Fig. 5. Stress distribution at 70° of flexion and magnified views of the flexion region on the xz plane for (a) pure silicone, (b) S1, and (c) S2 composite samples, and (d) stress distribution at different flexion and extension angles.

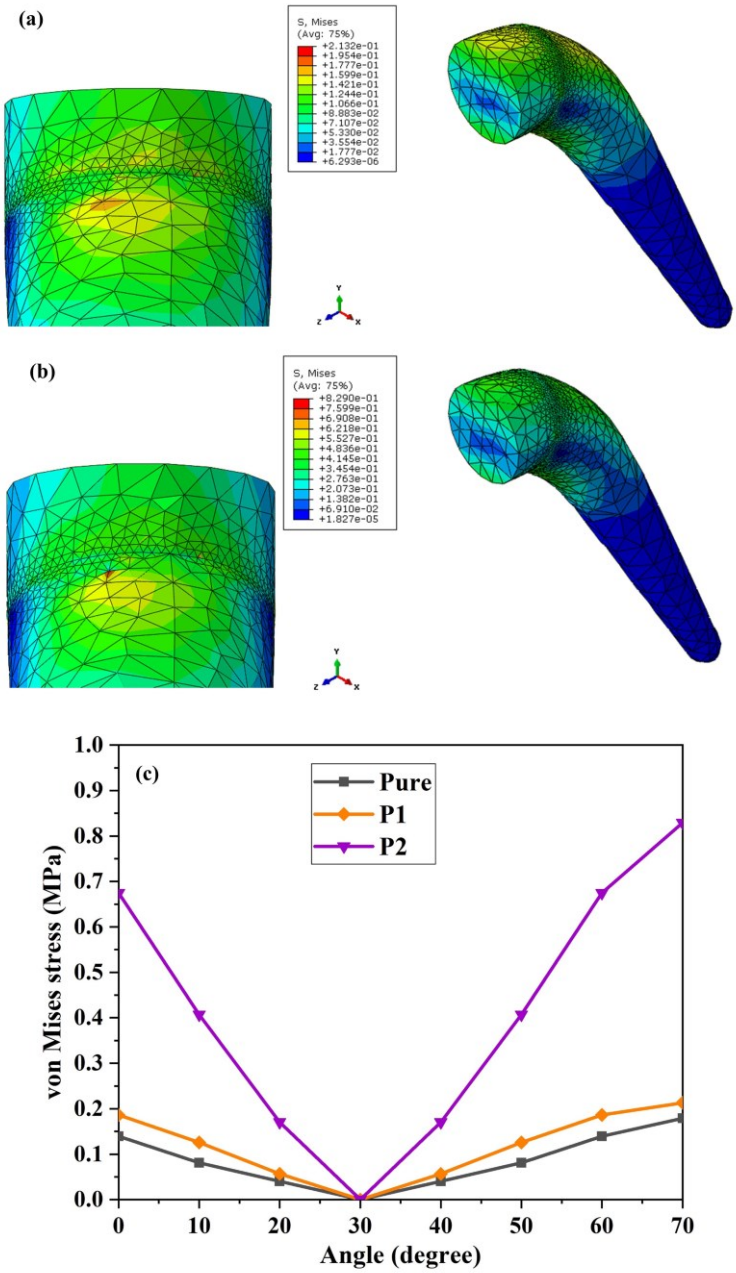


Fig. 6. Stress distribution at 70° of flexion and magnified views of the flexion region on the xz plane for (a) P1 and (b) P2 composite samples, and (c) stress distribution at different flexion and extension angles.

As reported in previous studies, the P2 composite is stronger than the S2 composite, whereas the hybrid composite (SP) exhibits intermediate behavior. This result should not be interpreted as evidence that these materials are mechanically inferior. In a displacement-controlled simulation, the joint angle is imposed regardless of material stiffness. A stiffer material therefore develops a greater internal reaction to accommodate the same prescribed deformation. The stress increase is consequently a direct consequence of the boundary condition and the constitutive response.

3.2. Stress distribution during flexion

In the next part of this study, a load of 0.5 N was applied to the implants, and the resulting stress and strain, flexion angle, and displacement were measured. The results are shown in Table 3. These measurements are used for comparing the mechanical performance of the implant materials.

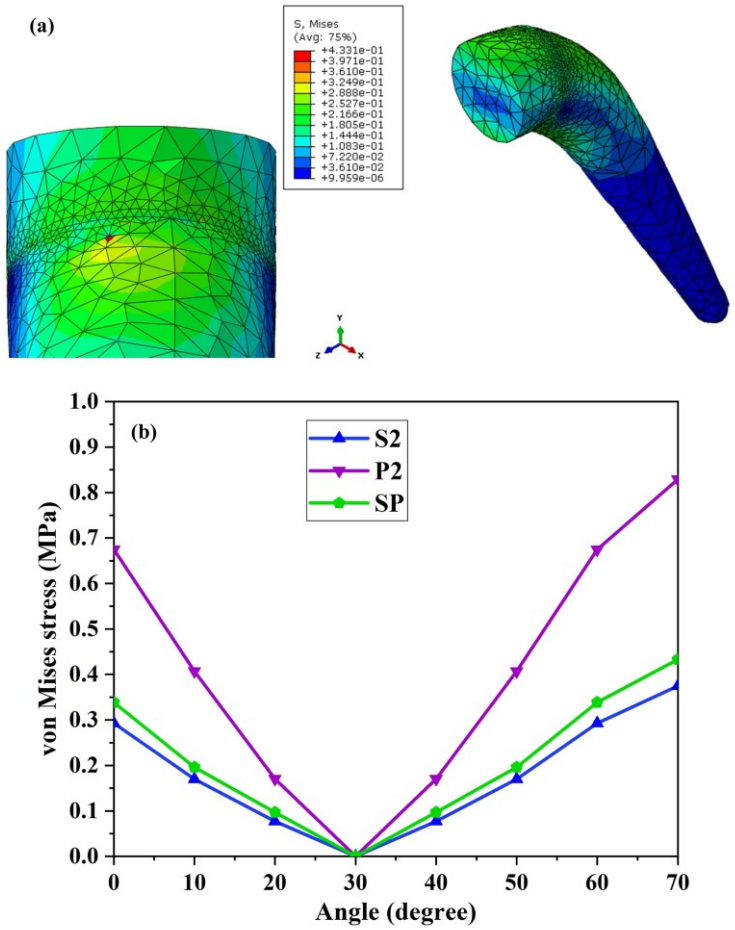


Fig. 7. Stress distribution at 70° of flexion and a magnified view of the flexion region on the xz plane for (a) the SP hybrid silicone rubber composite, and (b) comparison of stress distributions at different flexion and extension angles for the hybrid and single-reinforcement composite implants.

Table 3. Parameters measured under an applied load of 0.5 N for all implant samples

Reinforcement	Pure	S1	S2	P1	P2	SP
Angle	61.48	61.35	33.05	41.83	13.64	27.21
Displacement	12.92	12.85	7.12	9.2	3.31	6.19
Strain	0.41	0.4	0.21	0.28	0.11	0.2
Stress (MPa)	0.55	0.53	0.374	0.39	0.33	0.372

The most important observation is that the ranking of stress under the constant-load condition differs from the stress ranking observed during prescribed flexion. This apparent difference is not contradictory. Under the 70° flexion simulations, deformation is prescribed and the material response determines the reaction stress. Under the 0.5 N simulation, the force is prescribed, and the material response determines the resulting deformation. A more strongly reinforced composite therefore deforms less, resulting in lower strain and smaller geometric distortion. Because the hinge configuration is highly nonlinear, the reduction in deformation can also reduce the peak local stress. This explains why P2, despite experiencing relatively high stresses during prescribed flexion, produced the lowest peak stress under the force-controlled condition.

The particularly favorable response of P2 is consistent with the previous tensile characterization of the same material system [18]. PP fibers can improve load transfer through the silicone matrix and increase resistance to deformation. The present FEA extends that material-level observation to the implant scale; the

benefit of increased composite strength is expressed primarily as reduced displacement and strain under a fixed external load. From a biomechanical perspective, this is important because excessive implant deformation can alter the effective joint kinematics and may increase the amplitude of cyclic deformation during repeated use. Regions with higher stress are prone to crack initiation. Elastomer failure can occur due to fatigue, therefore, reducing stress may help extend implant life [18, 19].

3.3. Angle of flexion and displacement

The angle of flexion and displacement of implants are shown in Fig. 8 and Fig. 9. The main numerical results for von Mises stress, joint angle, and displacement have been presented in comparative graphical form in Fig. 10. As can be seen, flexion of the P2 composite is less than that of the other samples, and this angle increases as composite strength decreases (SP, S2, and pure silicon rubber, respectively). In samples with higher stiffness, flexion was lower and resistance to the applied load was greater, so the angle of flexion and displacement in stiffer samples were less than those in the others samples. Flexible samples, like pure silicone rubber, showed more displacement.

This result demonstrates the direct connection between material reinforcement and implant kinematics. A flexible silicone implant must deform sufficiently to permit finger movement, but excessive deformation may increase local strains and accelerate mechanical damage. Therefore, the design objective is not simply to maximize stiffness. Instead, an appropriate balance is required between flexibility and mechanical resistance. Excessive stiffness could restrict joint motion, whereas excessive compliance could increase deformation and local strain.

3.4. Stress and strain distribution

Stress and strain distribution are shown in Fig. 11 and Fig. 12. In stiffer sample implants, lower stress and strain are induced, and implant lifetime increases. As can be seen in Fig. 11, stiffer samples showed less flexion, and, as the results of the first part of the study showed, stress distribution increased with an increase in the flexion angle.

In the present model, under the applied 0.5 N load, the maximum strain was approximately 0.41 for pure silicone, 0.21 for S2, 0.11 for P2, and 0.20 for SP. Thus, the reinforced composites exhibited substantially lower deformation than pure silicone under the same external load. This behavior is consistent with their higher mechanical resistance as determined from the experimental characterization. The simulated maximum strain should be distinguished from the ultimate tensile strain obtained experimentally, because the former represents the local strain developed under the specific FE loading condition, whereas the latter represents the strain at failure during tensile testing. Therefore, the comparison provides an indication of the deformation level relative to the experimentally characterized material failure behavior. These values are below the ultimate tensile strain reported in the previous tensile characterization.

Overall, the results demonstrate that FEA can provide a useful bridge between the mechanical properties of silicone composites and their expected implant-level behavior. The results indicate that the mechanical response of the composites depends strongly on the loading condition and their constitutive stiffness. Under prescribed flexion, stiffer composites develop higher reaction stresses to accommodate the imposed deformation, whereas under a constant applied load, stiffer composites undergo less deformation and lower strain. Recognizing this distinction improves the mechanical interpretation of the simulations and provides a more rational basis for selecting reinforced silicone formulations for MCP joint arthroplasty.

The computation of load and stress in joints is complicated, and it is not easy to calculate the loads and stresses induced in metacarpophalangeal joints [20]. Therefore, experimental work is required, as Butz et al. [21] estimated joint stresses for simple daily activities.

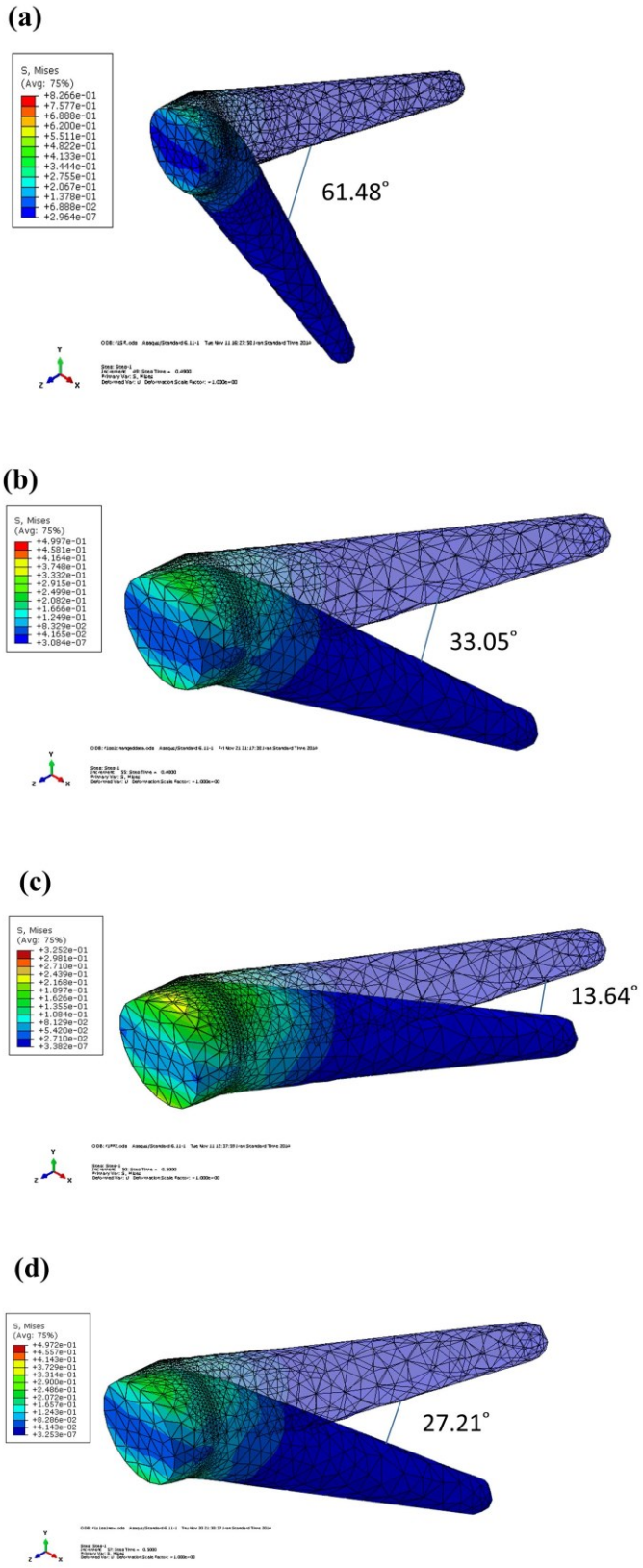


Fig. 8. Comparison of the initial and final positions of the implants and the corresponding flexion angles under an applied load of 0.5 N for (a) pure silicone, (b) S2, (c) P2, and (d) SP composite implants.

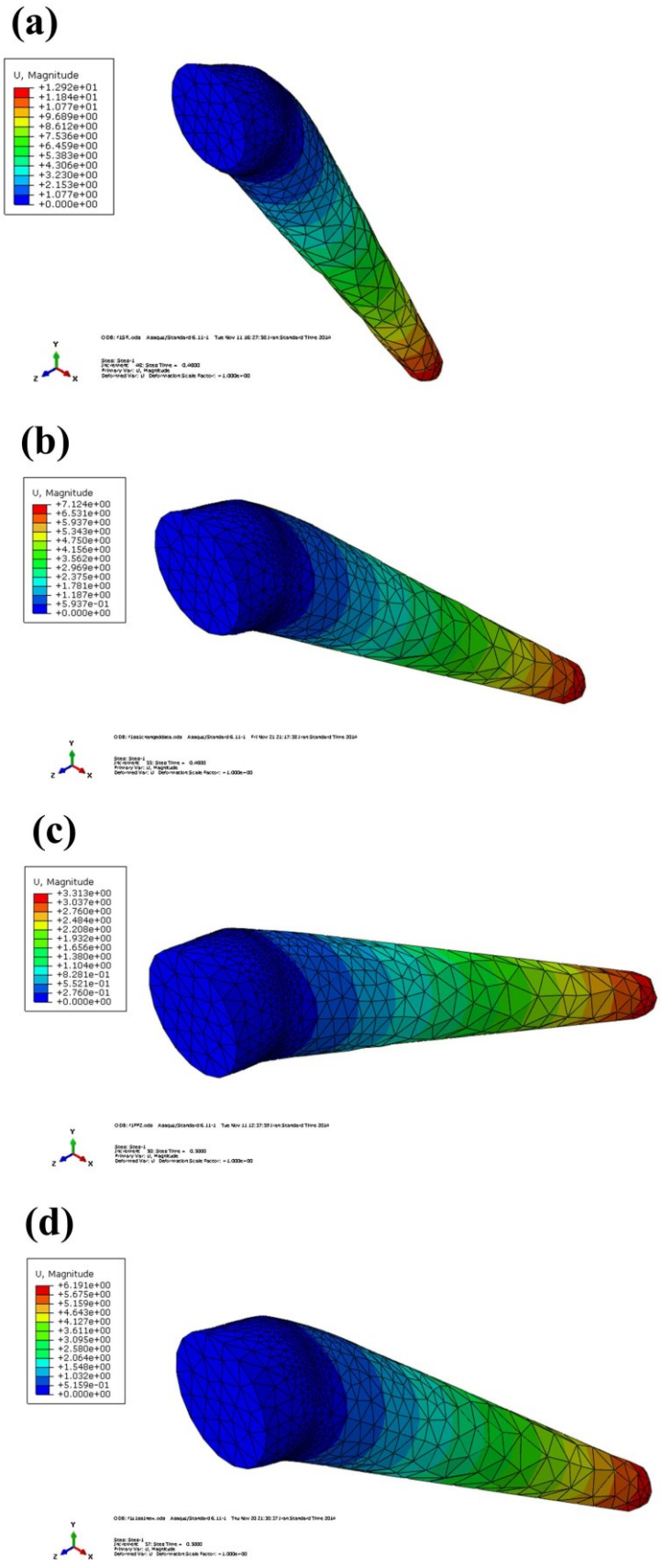


Fig. 9. Contours of total displacement magnitude (U) obtained from the FE analysis under an applied load of 0.5 N for (a) pure silicone, (b) S2, (c) P2, and (d) SP composite implants.

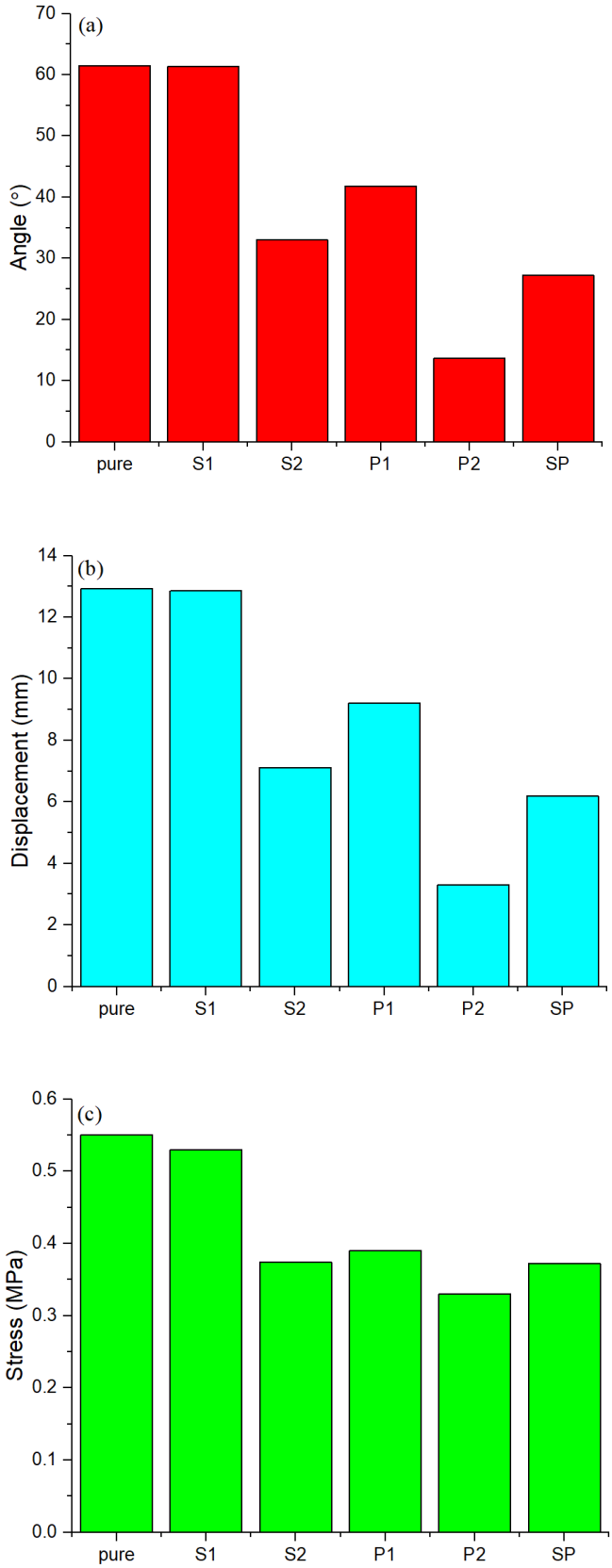


Fig. 10. von Mises stress, joint angle, and displacement of different samples.

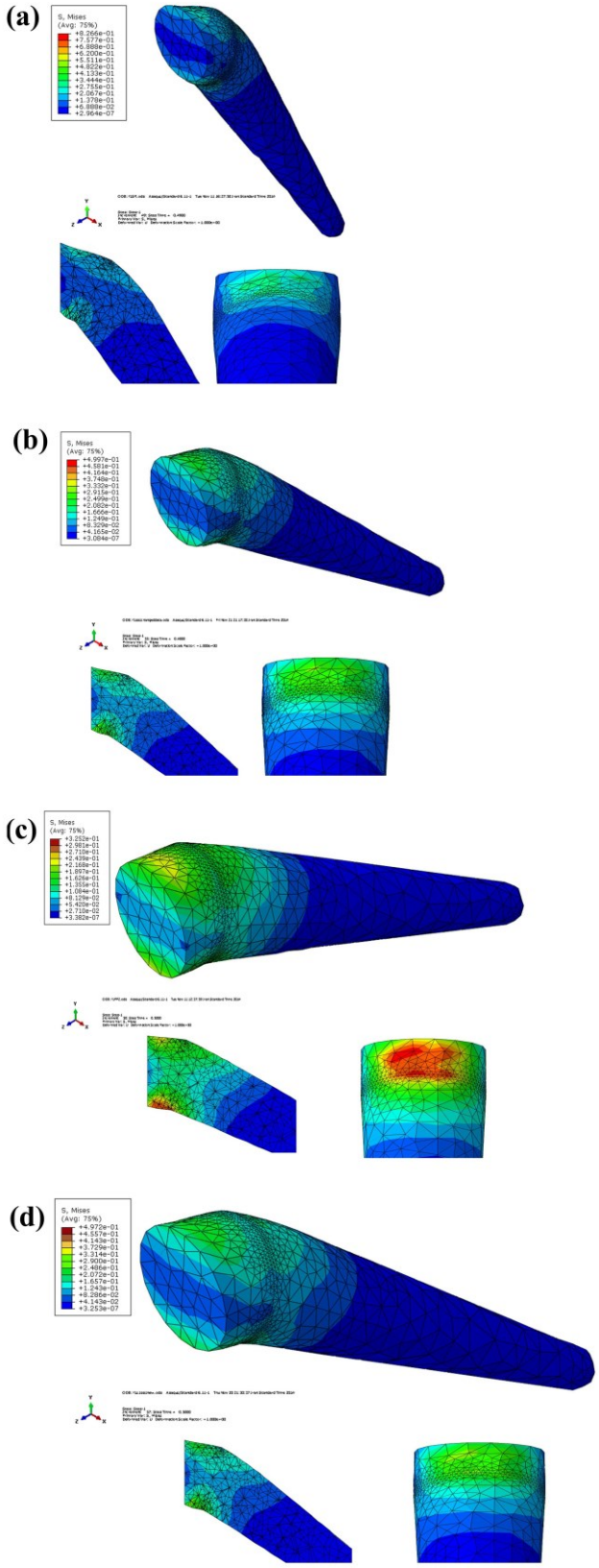


Fig. 11. von Mises stress distribution in the implants under an applied load of 0.5 N, including magnified views of the flexion region on the xz plane and cross-sectional views on the yz plane for (a) pure silicone, (b) S2, (c) P2, and (d) SP composite implants.

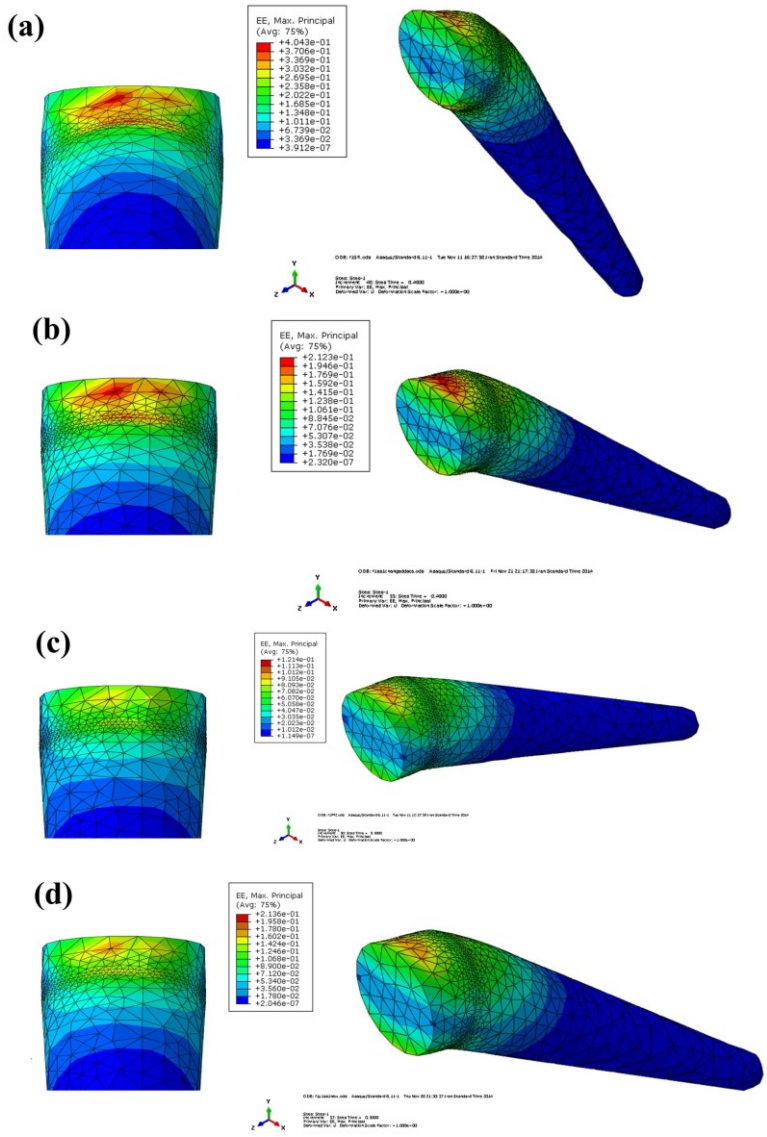


Fig. 12. Strain distribution under an applied load of 0.5 N in the implant and magnified view of the flexion region in the xz plane for (a) pure, (b) S2, (c) P2, and (d) SP composites.

4. Conclusion

The metacarpophalangeal joint is one of the most important joints, and it may sometimes need to be replaced with implants when necessary. To better understand implant biomechanics and service life, finite element analysis seems to be vital, and in this study, different materials used for finger joint implants were compared using simulation.

1) Stress concentration in the central regions is greater than that in other regions, and stress increased with an increase in the angle of flexion.

2) Composite samples with 2 wt.% PP and 1 wt.% SiO_2/1 wt.% PP, which have greater strength, showed greater resistance to a 0.5 N load, and exhibited less flexion and displacement.

3) Stress and strain in implants with greater strength were lower than those in the other implants under the applied-load condition, and this may contribute to longer implant life. P2 showed the greatest resistance to deformation, with the lowest displacement (3.31), strain (0.11), and stress (0.33 MPa) among the investigated formulations.

Comprehensive understanding of biomaterial properties and biomechanics can help guide the development of new joint materials and designs with better performance.

Authors' contributions

S. Ziraki: Conceptualization, Methodology, Investigation, Software, Visualization, Writing - original draft, Writing - review & editing

A. A. Ashraf: Software, Methodology

S. M. Zebarjad: Project administration, Supervision

M. J. Hadianfard: Project administration, Supervision

Conflict of interest

The author declares that there is no conflict of interest regarding in this research.

Funding

This research has not received any funding.

5. References

[1] Thoene, M., Bejer-Olenska, E., & Wojtkiewicz, J. (2023). The current state of osteoarthritis treatment options using stem cells for regenerative therapy: A review. *International Journal of Molecular Sciences*, *24*(10), 8925. https://doi.org/10.3390/ijms24108925

[2] Peck, J., Slovek, A., Miro, P., Vij, N., Traube, B., Lee, C., Berger, A. A., Kassem, H., Kaye, A. D., Sherman, W. F. & Abd-Elsayed, A. (2021). A Comprehensive review of viscosupplementation in osteoarthritis of the knee. *Orthopedic Reviews*, *13*(2), 1–11. https://doi.org/10.52965/001C.25549

[3] Biddiss, E. A., Bogoch, E. R., & Meguid, S. A. (2005). Three-dimensional finite element analysis of prosthetic finger joint implants. *International Journal of Mechanics and Materials in Design*, *1*(2004), 317–328. https://doi.org/10.1007/s10999-005-3308-3

[4] Vranis, N. M., Marascalchi, B., & Melamed, E. (2020). Trends in proximal interphalangeal and metacarpophalangeal joint arthroplasty utilization using statewide databases. *The Journal of Hand Surgery (Asian-Pacific Volume)*, *25*(01), 39–46. https://doi.org/10.1142/S2424835520500058

[5] Paesa, M., Alejo, T., Garcia-Alvarez, F., Arruebo, M., & Mendoza, G. (2023). New insights in osteoarthritis diagnosis and treatment: Nano-strategies for an improved disease management. *Wiley Interdisciplinary Reviews: Nanomedicine and Nanobiotechnology*, *15*(2), 1–35. https://doi.org/10.1002/wnan.1844

[6] Stokoe, S. M. (1990). *A finger function simulator and surface replacement prosthesis for the metacarpophalangeal joint*. Durham University.

[7] Koenuma, N., Ikari, K., Oh, K., Iwakura, N., & Okazaki, K. (2024). Long-term implant fracture rates following silicone metacarpophalangeal joint arthroplasty in rheumatoid arthritis. *Journal of Hand Surgery*, *49*(5), 443–449. https://doi.org/10.1016/j.jhsa.2024.01.009

[8] Iwamoto, T., Ishii, K., Suzuki, T., Kimura, H., Matsumura, N., & Sato, K. (2021). Risk factors contributing to early implant fracture in silicone metacarpophalangeal joint arthroplasty for patients with rheumatoid arthritis. *Journal of Hand Surgery*, *46*(3), 243.e1-243.e7. https://doi.org/10.1016/j.jhsa.2020.09.002

[9] Heller, M. O. (2022). Finite element analysis in orthopedic biomechanics. In *Human orthopaedic biomechanics* (pp. 637–658). Elsevier. https://doi.org/10.1016/B978-0-12-824481-4.00026-3

[10] Verma, A., Jain, A., Sekhar Sethy, S., Verma, V., Goyal, N., Vathulya, M., & Kandwal, P. (2024). Finite element analysis and its application in orthopaedics: A narrative review. *Journal of Clinical Orthopaedics and Trauma*, *58*, 102803. https://doi.org/10.1016/j.jcot.2024.102803

[11] Kadir, M. R. A., Kamsah, N., & Aminullah, M. A. (2008). Finite element study of metacarpophalangeal joint silicone implants. In *4th Kuala Lumpur International Conference on Biomedical Engineering* (pp. 420–423).

[12] S. Soman, M. A. (2011). Finite element analysis of fractured finger with Implant fixation using MIMICS. In *3rd International Conference on Electronics Computer Technology (ICECT)* (pp. 380–385).

[13] Completo, A., Semitela, A., Fonseca, F., & Nascimento, A. (2023). The silicone metacarpophalangeal joint arthroplasty: An in-vitro analysis. *Clinical Biomechanics*, *110*, 106120. https://doi.org/10.1016/j.clinbiomech.2023.106120

[14] Kim, Y. J., Bae, H. ah, & Hong, S. W. (2023). Biomechanical comparative finite element analysis between a conventional proximal interphalangeal joint flexible hinge implant and a novel implant design using a rolling contact joint mechanism. *Journal of Orthopaedic Surgery and Research*, *18*(1), 1–13. https://doi.org/10.1186/s13018-023-04477-y

[15] Pankaj, P. (2013). Patient-specific modelling of bone and bone-implant systems: the challenges. *International journal for numerical methods in biomedical engineering*, *29*(2), 233–249. https://doi.org/10.1002/cnm.2536

[16] Ziraki, S., Zebarjad, S. M., & Hadianfard, M. J. (2016). A study on the role of polypropylene fibers and silica nanoparticles on the compression properties of silicone rubber composites as a material of finger joint implant.

International Journal of Polymeric Materials and Polymeric Biomaterials, *66*(1), 48–52. https://doi.org/https:/doi.org/10.1080/00914037.2016.1180623

[17] Ziraki, S., Mojtaba, S., & Hadianfard, M. J. (2016). A study on the tensile properties of silicone rubber/polypropylene fibers/silica hybrid nanocomposites. *Journal of the Mechanical Behavior of Biomedical Materials*, *57*, 289–296. https://doi.org/10.1016/j.jmbbm.2016.01.019

[18] Pylios, T. (2010). *A new metacarpophalangeal joint replacement prosthesis*. University of Birmingham.

[19] Salamat, A. H., & Shepherd, D. E. T. (2010). Modelling silicone finger joint implant. In *17th Iranian Conference of Biomedical Engineering (ICBME)* (pp. 1–4).

[20] Hu, D., Howard, D., & Ren, L. (2014). Biomechanical analysis of the human finger extensor mechanism during isometric pressing. *Public Library of Science One*, *9*(4), e94533. https://doi.org/10.1371/journal.pone.0094533

[21] Butz, K. D., Merrell, G., & Nauman, E. A. (2012). A three-dimenional finite element analysis of finger joint stresses in the MCP joint while performing common tasks. *Hand*, *7*(3), 341–345. https://doi.org/10.1007/s11552-012-9430-4